Fast Inversion of Eddy Current Testing Data Through a Learning-by-Examples Approach for Robust Crack Localization

M. Salucci, N. Anselmi, G. Oliveri, and A. Massa

Abstract

This document presents a new learning-by-example (*LBE*) technique for the computationally-efficient inversion of eddy current testing (*ECT*) data in non-destructive testing and evaluation (*NDT-NDE*) scenarios. More precisely, the developed approach exploits a uniform sampling strategy to build a training set of input/output (*I/O*) pairs and exploits such information to train a Support Vector Regressor (SVR). During the *on-line* testing phase, previously-unseen *ECT* data are given as input to the trained model in order to predict the position of a single narrow crack within a planar conductive structure. Some representative numerical results are shown, in order to preliminarily assess the capabilities of the developed approach when dealing with the presence of a non-negligible amount of noise on test data.

1 Definitions

1.1 Notation

- a: a scalar value;
- $\mathbf{a}$: an L-dimensional row vector ($\mathbf{a} = \begin{bmatrix} a_1 & ... & a_{L-1} & a_L \end{bmatrix}$);
- $\mathbf{A}$: a $Q \times U$ matrix ($\mathbf{A} = \begin{bmatrix} a_{11} & ... & a_{1U} \\ \vdots & \ddots & \vdots \\ a_{Q1} & ... & a_{QU} \end{bmatrix}$);

1.2 List of Symbols

- I: number of crack parameters to estimate;
- $\mathbf{p}$: vector of crack parameters ($\mathbf{p} = \{p_1, p_2, ..., p_i, ..., p_I\}$);
- $\widetilde{\mathbf{p}}$: vector of estimated crack parameters ($\widetilde{\mathbf{p}} = \{\widetilde{p}_1, \widetilde{p}_2, ..., \widetilde{p}_i, ..., \widetilde{p}_I\}$)
- $\Phi\{.\}$: forward operator;
- $\Phi^{-1}\{.\}$: inverse operator;
- K: number of measurement points considered for the inversion;
- $\Phi\{\mathbf{p}\} = \{\Psi_k(\mathbf{p})\,;\, k = 1, ..., K\}$: set of complex-valued measurements associated to a given crack configuration $\mathbf{p}$;
- $\Psi_k(\mathbf{p}) = \Re\{\Psi_k(\mathbf{p})\} + j\Im\{\Psi_k(\mathbf{p})\}$: complex-valued measurement at point k;
- N: Number of training samples;
- $F = 2 \times K$: Total number of features for the inversion if both real and imaginary parts of each measurement point is considered;

1.3 Prediction Errors

In order to give a quantitative measure of the reconstruction accuracy obtained by the proposed inversion method, the following error metrics have been defined and will used for the successive numerical validation:

1. mean absolute error (MAE) over a set of M test samples

$$MAE\left(p_i\right) = \frac{1}{M}\sum_{m=1}^{M}\left|p_i^{(m)} - \widetilde{p}_i^{(m)}\right| \tag{1}$$

2. normalized mean error (NME) over a set of M test samples

$$NME\left(p_i\right) = \frac{1}{M}\sum_{m=1}^{M}\frac{\left|p_i^{(m)} - \widetilde{p}_i^{(m)}\right|}{\left|p_i^{(m)}\right|} \tag{2}$$

3. relative error (RE) for the m-th prediction

$$RE\left(p_i^{(m)}\right) = \frac{\left|p_i^{(m)} - \widetilde{p}_i^{(m)}\right|}{\left|p_i^{(m)}\right|} \times 100 \tag{3}$$

where

- p_i is the i-th estimated parameter (i.e., $p_1 = x_0$, $p_2 = y_0$ and $p_3 = z_0$);
- $p_i^{(m)}$ is the actual value of the i-th parameter associated to the m-th test sample;
- $\widetilde{p}_i^{(m)}$ is the predicted value of the i-th parameter associated to the m-th test sample.

1.4 Signal-to-Noise Ratio

In order to test the performances of the inversion procedure against noisy data, a complex additive white Gaussian noise ($AWGN$) has been superimposed on both training and test ECT measurements. More in details, the signal-to-noise ratio (SNR) of a given set of K measurements is defined as

$$SNR = 10log_{10}\left\{\frac{\sum_{k=1}^{K}\left|\Psi_k\right|^2}{\sum_{k=1}^{K}\left|n_k\right|^2}\right\} = 10log10\left\{\frac{\sum_{k=1}^{K}\left[\Re\left(\Psi_k\right)\right]^2 + \left[\Im\left(\Psi_k\right)\right]^2}{\sum_{k=1}^{K}\left[\Re\left(n_k\right)\right]^2 + \left[\Im\left(n_k\right)\right]^2}\right\} \tag{4}$$

where $n_k = \Re\left(n_k\right) + j\Im\left(n_k\right)$ is the complex noise added to the k-th measure.

2 LBE Inversion Approaches

2.1 Standard LBE Approach ($GRID - SVR$)

1. **Build a training set of N samples.**

   (a) Build a set $\mathbf{P}_N$ of N configurations of the crack (dim. $[N \times I]$) (e.g., positions within the plate)

$$\mathbf{P}_N = \begin{bmatrix} \mathbf{p}^{(1)} \\ \vdots \\ \mathbf{p}^{(N)} \end{bmatrix} = \begin{bmatrix} p_1^{(1)} & ... & p_I^{(1)} \\ \vdots & \ddots & \vdots \\ p_1^{(N)} & ... & p_I^{(N)} \end{bmatrix} = \begin{bmatrix} x_0^{(1)} & y_0^{(1)} & z_0^{(1)} \\ \vdots & \vdots & \vdots \\ x_0^{(N)} & y_0^{(N)} & z_0^{(N)} \end{bmatrix}$$

   using a uniform grid sampling in the I-dimensional space of crack parameters;

   (b) Use the forward solver $\Phi\{.\}$ to compute the ECT signal in K measurement points associated to the N configurations of the crack. Build the following matrix of measurements where real and imaginary parts of each measurement point are treated as separate real-valued features (dim. $[N \times 2K] = [N \times F]$)

$$\mathbf{\Psi}_N = \begin{bmatrix} \mathbf{\Psi}^{(1)} \\ \vdots \\ \mathbf{\Psi}^{(N)} \end{bmatrix} = \begin{bmatrix} \Re\{\Psi_1(\mathbf{p}^{(1)})\} & \Im\{\Psi_1(\mathbf{p}^{(1)})\} & ... & \Re\{\Psi_K(\mathbf{p}^{(1)})\} & \Im\{\Psi_K(\mathbf{p}^{(1)})\} \\ \vdots & & \ddots & & \vdots \\ \Re\{\Psi_1(\mathbf{p}^{(N)})\} & \Im\{\Psi_1(\mathbf{p}^{(N)})\} & ... & \Re\{\Psi_K(\mathbf{p}^{(N)})\} & \Im\{\Psi_K(\mathbf{p}^{(N)})\} \end{bmatrix};$$

   (c) The training set of N samples is then composed by the input-output pair

$$\{\mathbf{\Psi}_N; \mathbf{P}_N\}.$$

2. **Build a test set of M samples (different from the N training samples).**

   (a) Build a new set $\mathbf{P}_M$ of M configurations of the crack (dim. $[M \times I]$) (e.g., positions within the plate)

$$\mathbf{P}_M = \begin{bmatrix} \mathbf{p}^{(1)} \\ \vdots \\ \mathbf{p}^{(M)} \end{bmatrix} = \begin{bmatrix} p_1^{(1)} & ... & p_I^{(1)} \\ \vdots & \ddots & \vdots \\ p_1^{(M)} & ... & p_I^{(M)} \end{bmatrix} = \begin{bmatrix} x_0^{(1)} & y_0^{(1)} & z_0^{(1)} \\ \vdots & \vdots & \vdots \\ x_0^{(M)} & y_0^{(M)} & z_0^{(M)} \end{bmatrix}$$

   by sampling the I-dimensional space of crack parameters;

   (b) Use the forward solver $\Phi\{.\}$ to compute the ECT signal in K measurement points associated to the M test configurations of the crack. Build the following matrix of measurements where real and imaginary parts of each measurement point are treated as separate real-valued features (dim. $[M \times 2K] = [M \times F]$)

$$\mathbf{\Psi}_M = \left[\begin{array}{c} \mathbf{\Psi}^{(1)} \\ \vdots \\ \mathbf{\Psi}^{(M)} \end{array}\right] = \left[\begin{array}{ccccc} \Re\left\{\Psi_1\left(\mathbf{p}^{(1)}\right)\right\} & \Im\left\{\Psi_1\left(\mathbf{p}^{(1)}\right)\right\} & ... & \Re\left\{\Psi_K\left(\mathbf{p}^{(1)}\right)\right\} & \Im\left\{\Psi_K\left(\mathbf{p}^{(1)}\right)\right\} \\ \vdots & & \ddots & & \vdots \\ \Re\left\{\Psi_1\left(\mathbf{p}^{(M)}\right)\right\} & \Im\left\{\Psi_1\left(\mathbf{p}^{(M)}\right)\right\} & ... & \Re\left\{\Psi_K\left(\mathbf{p}^{(M)}\right)\right\} & \Im\left\{\Psi_K\left(\mathbf{p}^{(M)}\right)\right\} \end{array}\right];$$

3. **Support Vector Regression (SVR).**

Since traditional SVRs are able to manage only single-dimensional outputs, a separate SVR is considered for each parameter of the defect to estimate. For a given training dimension N and for each i-th parameter of the crack to estimate ($i = 1, ..., I$):

(a) Train a SVR using a training set composed as

$$\left\{\mathbf{\Psi}_N; \mathbf{P}_{N,i}\right\} = \left\{\left[\begin{array}{ccccc} \Re\left\{\Psi_1\left(\mathbf{p}^{(1)}\right)\right\} & \Im\left\{\Psi_1\left(\mathbf{p}^{(1)}\right)\right\} & ... & \Re\left\{\Psi_K\left(\mathbf{p}^{(1)}\right)\right\} & \Im\left\{\Psi_K\left(\mathbf{p}^{(1)}\right)\right\} \\ \vdots & & \ddots & & \vdots \\ \Re\left\{\Psi_1\left(\mathbf{p}^{(N)}\right)\right\} & \Im\left\{\Psi_1\left(\mathbf{p}^{(N)}\right)\right\} & ... & \Re\left\{\Psi_K\left(\mathbf{p}^{(N)}\right)\right\} & \Im\left\{\Psi_K\left(\mathbf{p}^{(N)}\right)\right\} \end{array}\right]; \left[\begin{array}{c} p_i^{(1)} \\ \vdots \\ p_i^{(N)} \end{array}\right]\right\}$$

where $\mathbf{P}_{N,i}$ is the i-th column of $\mathbf{P}_N$;

(b) Test the SVR giving it as input the matrix of new test measurements $\mathbf{\Psi}_M$. As output, the SVR will produce a vector of M estimated values for the i-th parameter

$$\widetilde{\mathbf{P}}_{M,i} = \left[\begin{array}{c} \widetilde{p}_i^{(1)} \\ \vdots \\ \widetilde{p}_i^{(M)} \end{array}\right].$$

3 Problem 1: Crack Location Estimation Inside a Plate Structure

3.1 Description

Let be given an homogeneous plate of thickness T and conductivity σ affected by a narrow crack and inspected by a single coil working in absolute mode at frequency f with lift-off δ (Fig. 1). The location of the crack is completely described by the vector $\mathbf{p}$ of $I = 3$ parameters

$$\mathbf{p} = \{x_0, y_0, z_0\} \tag{5}$$

which correspond to the coordinates of its barycentre (Fig. 1). Moreover, we assume that the dimensions of the crack are fixed, known and completely described by the values of its depth (d_0), width (w_0) and length (l_0), respectively (Fig. 1).

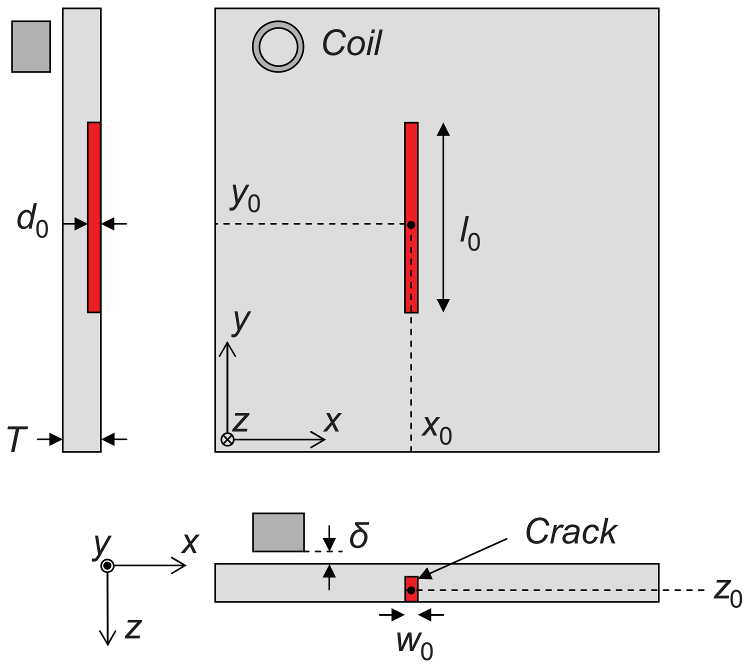

Figure 1: Geometry of the problem.

A metamodel is used as forward solver to compute in a fast but accurate way the measured *ECT* signal associated to a particular position of the defect. More in details, for a given vector $\mathbf{p}$ of crack coordinates, the metamodel computes the complex *ECT* signal over a set of K measurement points uniformly distributed on the (x, y) plane

$$\mathbf{\Psi} = \Phi\{\mathbf{p}\} = \{\Psi_k;\, k = 1, ..., K\} \tag{6}$$

where

- $\Psi_k = \Re\{\Psi_k\} + j\Im\{\Psi_k\}$ is the complex-valued *ECT* signal collected by the k-th measurement point (i.e., the impedance variation on the coil);

- $\Phi\{.\}$ is the forward operator, linking the defect barycentre ($\mathbf{p}$) to the collected *ECT* signal ($\mathbf{\Psi}$).

The goal of the inverse problem is to retrieve an estimation of the (unknown) position of the flaw $\widetilde{\mathbf{p}} = \{\widetilde{x}_0, \widetilde{y}_0, \widetilde{z}_0\}$ (i.e., the output space) by exploiting the information embedded inside $\mathbf{\Psi}$ (i.e., the input space). Such a problem can be formulated as follows

$$\widetilde{\mathbf{p}} = \Phi^{-1}\{\mathbf{\Psi}\} \tag{7}$$

where $\Phi^{-1}\{.\}$ denotes the (unknown) inverse operator, that has to be estimated.

3.2 Parameters of the forward solver (fixed)

- **Forward solver**
  - total number of measurement points along x (i.e., across the crack): $H_x = 41$;
  - measurement step along x: $\Delta_x = 0.5$ [mm];
  - total extension of the measurement region along x: $L_x = 20.0$ [mm];
  - total number of measurement points along y (i.e., along the crack): $H_y = 57$;
  - measurement step along y: $\Delta_y = 0.5$ [mm];
  - total extension of the measurement region along y: $L_y = 28.0$ [mm];
  - total number of measurement point computed by the forward solver: $H = H_x \times H_y = 2337$;

Plate	
Thickness T	1.55 [mm]
Conductivity σ	1.02 [MS/m]
Coil	
Inner radius r_1	1.0 [mm]
Outer radius r_2	1.75 [mm]
Length l_c	2.0 [mm]
Number of turns n_t	328
Lift-off δ	0.303 [mm]
Frequency f	100.0 [KHz]
Crack	
Depth d_0	0.62 [mm] (40% of T)
Length l_0	10.0 [mm]
Width w_0	0.3 [mm]

Table 1: Fixed parameters.

Parameter	**Min [mm]**	**Max [mm]**
Crack x-coordinate x_0	5.0	25.0
Crack y-coordinate y_0	1.0	29.0
Crack z-coordinate z_0	0.93	1.24

Table 2: Validity ranges of the forward meta-model.

3.3 Standard LBE Approach $(GRID - SVR)$: Performances

3.3.1 Parameters

- **Measurement set-up for the inversion**
  - considered measurement step: $\Delta_x = \Delta_y = 1.0$ [mm];
  - number of considered measurement points $K = K_x \times K_y = 21 \times 29 = 609$;
  - measured quantity for each k-th point: $\{\Re(\Psi_k), \Im(\Psi_k)\}$;
  - total number of measured features: $F = 2 \times K = 1218$;

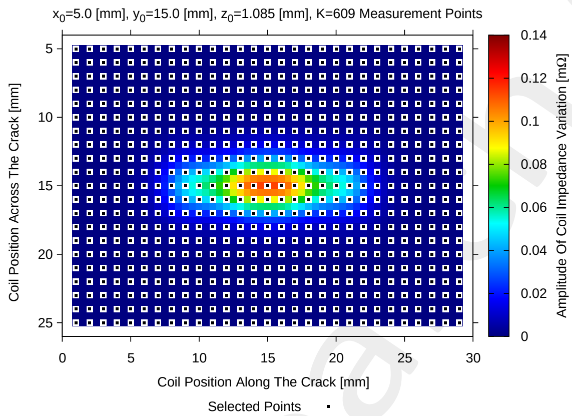

Figure 2: Location of the measurement points selected for the inversion ($K = 609$).

- **Standard LBE Approach**
  - Training set generation
    - sampling: uniform grid sampling in (x_0, y_0, z_0);
    - number of quantization levels: $Q_{x_0} = Q_{y_0} = Q_{z_0} = \{5; 6; ...; 10\}$;
    - number of training samples: $N = Q_{x_0} \times Q_{y_0} \times Q_{z_0} = \{125; 216; ...; 1000\}$;
    - SNR on training data: Noiseless;
  - Test set generation
    - Sampling: Latin Hypercube Sampling (LHS);
    - Number of test samples: $M = 1000$;
    - SNR on test data: Noiseless + $SNR = \{40; 30; 20; 10\}$ [dB].

3.3.2 True vs. Predicted ($SNR = 20$ [dB])

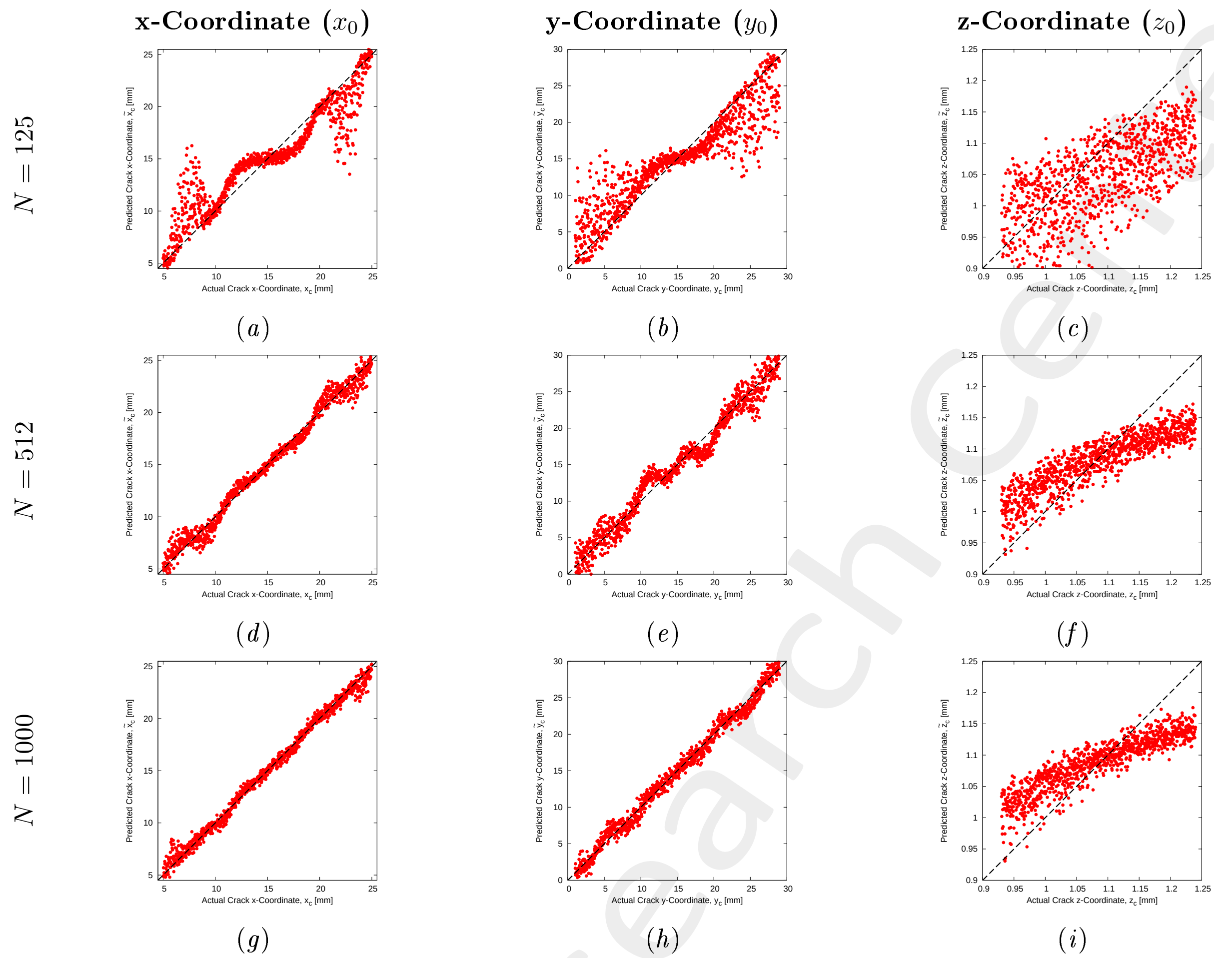

Figure 3: **Standard Approach -** True vs. predicted crack coordinates for different dimensions of the training set (N). $SNR = 20$ [dB] on test ECT data.

3.3.3 Errors

x-Coordinate (x_0) **y-Coordinate** (y_0) **z-Coordinate** (z_0)

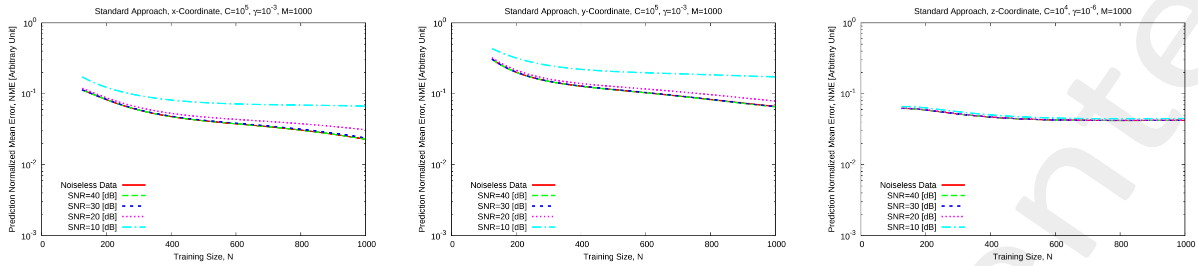

(a) (b) (c)

Figure 4: **Standard Approach** - Normalized Mean Error (NME) vs. training size (N)

x-Coordinate (x_0) **y-Coordinate** (y_0) **z-Coordinate** (z_0)

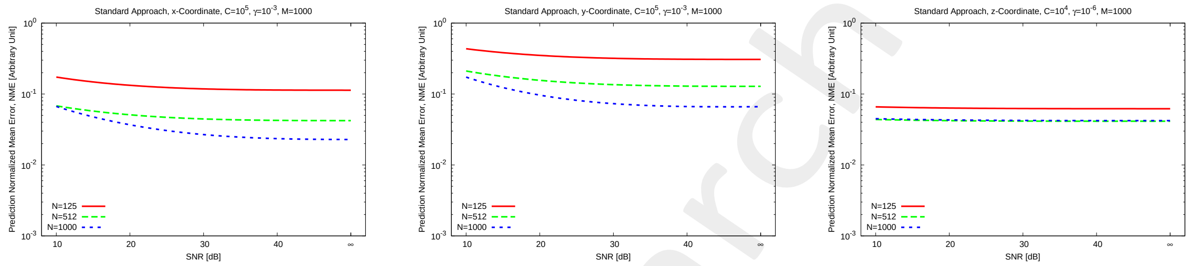

(a) (b) (c)

Figure 5: **Standard Approach** - Normalized Mean Error (NME) vs. SNR on the test ECT measurements.

References

[1] M. Salucci, N. Anselmi, G. Oliveri, P. Calmon, R. Miorelli, C. Reboud, and A. Massa, "Real-time NDT-NDE through an innovative adaptive partial least squares SVR inversion approach," *IEEE Trans. Geosci. Remote Sens.*, vol. 54, no. 11, pp. 6818-6832, Nov. 2016.

[2] M. Salucci, G. Oliveri, F. Viani, R. Miorelli, C. Reboud, P. Calmon, and A. Massa, "A learning-by-examples approach for non-destructive localization and characterization of defects through eddy current testing measurements," in *2015 IEEE International Symposium on Antennas and Propagation*, Vancouver, 2015, pp. 900-901.

[3] M. Salucci, S. Ahmed and A. Massa, "An adaptive Learning-by-Examples strategy for efficient Eddy Current Testing of conductive structures," in *2016 European Conference on Antennas and Propagation*, Davos, 2016, pp. 1-4.

[4] P. Rocca, M. Benedetti, M. Donelli, D. Franceschini, and A. Massa, "Evolutionary optimization as applied to inverse problems," *Inverse Probl.*, vol. 25, pp. 1-41, Dec. 2009.

[5] A. Massa, P. Rocca, and G. Oliveri, "Compressive sensing in electromagnetics - A review," *IEEE Antennas Propag. Mag.*, pp. 224-238, vol. 57, no. 1, Feb. 2015.

[6] N. Anselmi, G. Oliveri, M. Salucci, and A. Massa, "Wavelet-based compressive imaging of sparse targets," *IEEE Trans. Antennas Propag.*, vol. 63, no. 11, pp. 4889-4900, Nov. 2015.

[7] M. Salucci, G. Oliveri, and A. Massa, "GPR prospecting through an inverse-scattering frequency-hopping multifocusing approach," *IEEE Trans. Geosci. Remote Sens.*, vol. 53, no. 12, pp. 6573-6592, Dec. 2015.

[8] T. Moriyama, G. Oliveri, M. Salucci, and T. Takenaka, "A multi-scaling forward-backward time-stepping method for microwave imaging," *IEICE Electron. Express*, vol. 11, no. 16, pp. 1-12, Aug. 2014.

[9] T. Moriyama, M. Salucci, M. Tanaka, and T. Takenaka, "Image reconstruction from total electric field data with no information on the incident field," *J. Electromagnet. Wave.*, vol. 30, no. 9, pp. 1162-1170, 2016.

[10] M. Salucci, L. Poli, and A. Massa, "Advanced multi-frequency GPR data processing for non-linear deterministic imaging," *Signal Processing - Special Issue on "Advanced Ground-Penetrating Radar Signal-Processing Techniques,"* vol. 132, pp. 306-318, Mar. 2017.